

Duality in semi-inclusive pion electroproduction

F. E. Close

Rudolf Peierls Centre for Theoretical Physics, University of Oxford, 1 Keble Road, Oxford OX1 3NP, United Kingdom

W. Melnitchouk

Jefferson Lab, 12000 Jefferson Avenue, Newport News, Virginia 23606, USA

(Received 24 February 2009; published 8 May 2009)

We explore quark-hadron duality in semi-inclusive pion electroproduction on proton and neutron targets. Using the spin-flavor symmetric quark model, we compute ratios of π^+ and π^- cross sections for both unpolarized and polarized scattering and discuss realizations of duality in several symmetry-breaking scenarios. The model calculations allow one to understand some of the key features of recent data on semi-inclusive pion production at low energies.

DOI: [10.1103/PhysRevC.79.055202](https://doi.org/10.1103/PhysRevC.79.055202)

PACS number(s): 13.60.Hb, 13.87.Fh, 12.40.Nn, 12.39.Jh

I. INTRODUCTION

Quark-hadron duality in structure functions (also known as Bloom-Gilman duality [1]) is a well-established empirical phenomenon, relating measurements in the deep inelastic region to averages over nucleon resonances (for a review see Ref. [2]). Although a quantitative understanding of its origin in quantum chromodynamics (QCD) remains elusive, some insight into the possible realization of duality has recently been achieved through phenomenological model calculations [3–5].

For inclusive structure functions, Close and Isgur [3] showed how incorporation of spin-flavor SU(6) symmetry gives quantitative comparisons between the inelastic structure functions at high energies for proton or neutron targets and lower-energy data covering the resonance region. In particular, it was shown that an essential element in the appearance of duality was a pattern of constructive and destructive interference that suppressed multi-quark correlations, leaving only incoherent contributions from single quark scattering [3]. In the SU(6) model this was realized by summing over neighboring positive- and negative-parity excited states in the **56** and **70** multiplets, respectively.

When comparing with phenomenology, predictions based on SU(6) symmetry may be expected to be valid at quark momentum fractions $x \sim 1/3$ but are known to break down at larger x . Explicit symmetry-breaking scenarios, reflecting different patterns in the flavor-spin dependence of interquark forces, were considered in Ref. [6], and several of these were found to be consistent with duality. The SU(6)-breaking analysis extended the range of x up to $x \sim 1$ and identified implications for the high Q^2 behavior of the $N \rightarrow N^*$ transition form factors.

Recently, experimental investigations of duality have been carried out in charged pion electroproduction from proton and deuteron targets [7,8], measuring the ratios of semi-inclusive π^+ to π^- production as a function of $z \equiv E_\pi/\nu$, where ν is the energy transfer to the target. The data showed a smooth behavior in z , consistent with that observed by the HERMES [9] and European Muon Collaborations (EMC) [10] at higher energies, raising the question of whether a similar duality may be at play as that observed in inclusive structure functions [2].

In fact, a preliminary investigation of duality in semi-inclusive pion production was made in Ref. [3], where a factorization between structure and fragmentation functions was found to hold by summing over N^* resonances in the quark model. Ratios of π^+/π^- yields were calculated for unpolarized cross sections from protons and neutrons in the SU(6) limit, applicable at $x \sim 1/3$, and the sum over these was shown to reproduce the inclusive structure function results. Duality in semi-exclusive hard pion photoproduction was also considered in Ref. [11] for fixed center of mass scattering angles. The applicability of duality for pion photoproduction in specific kinematic regions was discussed in Ref. [12]. With the advent of the new semi-inclusive data in the resonance region and beyond [7,8], it is timely therefore to revisit this problem by extending the earlier work to the more realistic case of SU(6)-breaking and spin-dependent as well as spin-independent cross sections.

In this article we present a detailed account of the semi-inclusive pion production within a resonance excitation picture and evaluate the extent to which quark-hadron duality is realized in the data. In Sec. II we review the quark-parton model expectations for semi-inclusive cross-section ratios in the valence quark region. The main results of this study, namely the cross sections in terms of transitions to excited state resonances, are presented in Sec. III. We consider both the spin-flavor symmetric case, as well as several symmetry-breaking scenarios, and test the validity of duality for each scenario. The full set of matrix elements for the transitions $\gamma N \rightarrow N_1^* \rightarrow \pi N_2^*$, as well as an explicit example of a typical matrix element computation, are listed in the Appendices. Comparisons with recent semi-inclusive pion production data from Jefferson Lab and elsewhere are discussed in Sec. IV, where we generalize our to include nonleading fragmentation. Finally, some conclusions and ideas for future work outlined in Sec. V.

II. PARTON MODEL FRAGMENTATION

If the hadronization process is independent of the target, the semi-inclusive cross section can be factorized into a product of a parton distribution function describing the hard

scattering from a parton in the target, and the probability of the struck parton fragmenting into a specific hadron, parameterized by the fragmentation function. At the quark level, the semi-inclusive cross section for the production of pions from a nucleon target in the valence quark region ($x \gtrsim 0.3$) is proportional (at leading order in α_s) to

$$\mathcal{N}_N^\pi(x, z) = e_u^2 u^N(x) D_u^\pi(z) + e_d^2 d^N(x) D_d^\pi(z), \quad (1)$$

where $e_u(e_d) = 2/3(-1/3)$ is the $u(d)$ quark charge, q^N is the distribution of quarks q in the nucleon N with light-cone momentum fraction x , and D_q^π is the fragmentation function for quark q to produce a pion with energy fraction $z = E_\pi/\nu$, with E_π the pion energy and ν the energy transfer to the target. In both the distribution functions and fragmentation functions we have suppressed the explicit dependence on the scale Q^2 .

The fragmentation functions are traditionally separated into favored and disfavored classes, $D_u^{\pi^+} = D_d^{\pi^-} \equiv D$ and $D_d^{\pi^+} = D_u^{\pi^-} \equiv \bar{D}$, respectively, where we have further assumed isospin symmetry in relating the fragmentation functions for π^+ and π^- . In the leading fragmentation approximation, valid in the limit $z \rightarrow 1$, the hadronization process is dominated by the favored fragmentation, and $\bar{D} \rightarrow 0$. In this approximation the cross sections for proton and neutron targets can be written as:

$$\mathcal{N}_p^{\pi^+}(x, z) = e_u^2 u(x) D(z), \quad (2a)$$

$$\mathcal{N}_p^{\pi^-}(x, z) = e_d^2 d(x) D(z), \quad (2b)$$

$$\mathcal{N}_n^{\pi^+}(x, z) = e_u^2 d(x) D(z), \quad (2c)$$

$$\mathcal{N}_n^{\pi^-}(x, z) = e_d^2 u(x) D(z), \quad (2d)$$

where the quark distributions are defined to be those in the proton.

Similarly for a polarized target, the spin-dependent cross section can be written (at leading order) in terms of spin-dependent distribution functions Δq and corresponding fragmentation functions ΔD ,

$$\Delta \mathcal{N}_N^\pi(x, z) = e_u^2 \Delta u^N(x) \Delta D_u^\pi(z) + e_d^2 \Delta d^N(x) \Delta D_d^\pi(z). \quad (3)$$

Because the quark spins in a pion must average to zero, for pion production one expects the fragmentation functions to be independent of the polarization of the fragmenting quark, so that $\Delta D_q^\pi = D_q^\pi$.

If the quark distributions and fragmentation functions factorize as in Eq. (1), one can construct ratios of π^- to π^+ yields on the neutron and proton that are given by simple ratios of quark charges,

$$\frac{\mathcal{N}_n^{\pi^+}}{\mathcal{N}_p^{\pi^+}} = \frac{\mathcal{N}_p^{\pi^-}}{\mathcal{N}_n^{\pi^-}} = \frac{e_u^2}{e_d^2} = 4. \quad (4)$$

Similarly for the spin-dependent cross sections, one finds the model-independent relations:

$$\frac{\Delta \mathcal{N}_n^{\pi^+}}{\Delta \mathcal{N}_p^{\pi^+}} = \frac{\Delta \mathcal{N}_p^{\pi^-}}{\Delta \mathcal{N}_n^{\pi^-}} = 4. \quad (5)$$

This will serve as useful consistency checks on the duality between the partonic and hadronic descriptions of the semi-inclusive cross sections in the following section.

III. RESONANCE TRANSITIONS

In this section we describe the semi-inclusive production of pions using a hadronic basis within the SU(6) quark model, generalizing the discussion of Refs. [3,6] on inclusive structure functions. In the earlier work [3,6], the SU(6) model served as a useful framework in allowing one to visualize the underlying principles of quark-hadron duality and to provide a reasonably close contact with structure function phenomenology. As pointed out by Close and Isgur [3], duality between structure functions represented by (incoherent) parton distributions and by a (coherent) sum of squares of form factors can be achieved by summing over neighboring odd- and even-parity states. In the SU(6) model this is realized by summing over states in the $\mathbf{56}^+(L=0, \text{ even parity})$ and $\mathbf{70}^-(L=1, \text{ odd parity})$ multiplets, with each representation weighted equally.

For semi-inclusive scattering, pion production cross sections are constructed by summing coherently over excited nucleon resonances (N_1^*) in the s -channel intermediate state and in the final state (N_2^*) of $\gamma N \rightarrow N_1^* \rightarrow \pi N_2^*$, where both N_1^* and N_2^* belong to the $\mathbf{56}^+$ and $\mathbf{70}^-$ multiplets. Duality is then demonstrated by comparing the hadronic-level results with those of the parton model in Sec. II.

To generalize the model to values of x away from $x \sim 1/3$, where SU(6) symmetry is expected to be valid, we incorporate various SU(6)-breaking mechanisms, along the lines of those discussed in Ref. [6]. We recall that at the quark level, explicit SU(6)-breaking mechanisms produce different weightings of components of the initial-state wave function, which in turn induces different x dependences for the spin and flavor distributions. However, at the hadronic level SU(6) breaking in the matrix elements leads to suppression of transitions to specific N_1^* and N_2^* resonances, while starting from a symmetric SU(6) wave function for the initial state N .

A. SU(6) symmetric model

The amplitudes for the transitions $\gamma N \rightarrow N_1^*$ correspond to the absorption of a transversely polarized photon ($J_z = +1$), exciting the nucleon to a state N_1^* with total angular momentum $J_z = 1/2(3/2)$ described by the helicity amplitude $A_{1/2(3/2)}$. As in Refs. [3,6,13], we assume the interaction operator to be magnetic spin-flip, $\sum_i e_i \sigma_i^+$, where e_i is the charge of the i -th quark and $\sigma^+ = (\sigma_x + i\sigma_y)/2$ is the Pauli spin raising operator, as appropriate in the deep inelastic limit [14]. (This corresponds to the “ B ” terms in Ref. [15].)

For the pion emission operator we use leading term from Ref. [15] proportional to $\sum_i \tau_i^\pm \sigma_{zi}$ for π^\mp emission, where τ_i^\pm is the isospin raising/lowering operator (for the most general form of the operator see Ref. [15]). The leading operator is in fact general for unpolarized scattering, but for spin-dependent transitions it implicitly assumes that the emitted pion is collinear (or with $L_z = 0$), which is strictly valid only in the $z \rightarrow 1$ limit. For simplicity we retain this form in the present

TABLE I. Relative spin-averaged (spin-dependent) probabilities $\mathcal{N}_N^\pi (\Delta\mathcal{N}_N^\pi)$ for the $\gamma N \rightarrow N_1^* \rightarrow \pi N_2^*$ transitions in the SU(6) symmetric quark model, after summing over all intermediate states N_1^* .

	N_2^*					Sum
	28, 56⁺	410, 56⁺	28, 70⁻	48, 70⁻	210, 70⁻	
$\gamma p \rightarrow \pi^+ N_2^*$	100 (100)	32 (-16)	64 (64)	16 (-8)	4 (4)	216 (144)
$\gamma p \rightarrow \pi^- N_2^*$	0 (0)	24 (-12)	0 (0)	0 (0)	3 (3)	27 (-9)
$\gamma n \rightarrow \pi^+ N_2^*$	0 (0)	96 (-48)	0 (0)	0 (0)	12 (12)	108 (-36)
$\gamma n \rightarrow \pi^- N_2^*$	25 (25)	8 (-4)	16 (16)	4 (-2)	1 (1)	54 (36)

exploratory study, whose primary aim is to demonstrate the workings of duality in semi-inclusive scattering. In addition, the currently available data are for unpolarized cross sections, and refinements of the model to investigate the polarization dependence as a function of z can be made in future when new spin-dependent data become available.

Within this framework, the probabilities of the $\gamma N \rightarrow \pi N_2^*$ transitions can be obtained from Tables III–VII in Appendix A by summing over the intermediate states N_1^* spanning the **56⁺** and **70⁻** multiplets. In Table I we list the relative spin-averaged \mathcal{N}_N^π and spin-dependent $\Delta\mathcal{N}_N^\pi$ semi-inclusive cross sections (scaled by a factor $9^2 = 81$) for the SU(6) symmetric case for specific N_2^* final states, together with the sum over the N_2^* states. In the hadronic language we define the yield as

$$\mathcal{N}_N^\pi(x, z) = \sum_{N_2^*} \left| \sum_{N_1^*} F_{\gamma N \rightarrow N_1^*}(Q^2, M_1^*) \mathcal{D}_{N_1^* \rightarrow N_2^* \pi}(M_1^*, M_2^*) \right|^2, \quad (6)$$

where $F_{\gamma N \rightarrow N^*}$ is the $\gamma N \rightarrow N^*$ transition form factor, which depends on the masses of the virtual photon and excited nucleon (M_1^*), and $\mathcal{D}_{N_1^* \rightarrow N_2^* \pi}$ is a function representing the decay $N_1^* \rightarrow \pi N_2^*$, where M_2^* is the invariant mass of the final state N_2^* .

Summing over the N_2^* states in the **56⁺** and **70⁻** multiplets in Table I, we arrive at the following ratios of unpolarized π^- to π^+ semi-inclusive cross sections:

$$\frac{\mathcal{N}_p^{\pi^-}}{\mathcal{N}_p^{\pi^+}} = \frac{1}{8}, \quad \frac{\mathcal{N}_n^{\pi^-}}{\mathcal{N}_n^{\pi^+}} = \frac{1}{2}, \quad (7)$$

while for the corresponding spin-dependent π^- to π^+ ratios we have:

$$\frac{\Delta\mathcal{N}_p^{\pi^-}}{\Delta\mathcal{N}_p^{\pi^+}} = -\frac{1}{16}, \quad \frac{\Delta\mathcal{N}_n^{\pi^-}}{\Delta\mathcal{N}_n^{\pi^+}} = -1. \quad (8)$$

For specific π^+ and π^- production, the ratios of spin-dependent to spin-averaged cross sections are:

$$\frac{\Delta\mathcal{N}_p^{\pi^+}}{\mathcal{N}_p^{\pi^+}} = \frac{2}{3}, \quad \frac{\Delta\mathcal{N}_p^{\pi^-}}{\mathcal{N}_p^{\pi^-}} = -\frac{1}{3}, \quad (9a)$$

$$\frac{\Delta\mathcal{N}_n^{\pi^+}}{\mathcal{N}_n^{\pi^+}} = -\frac{1}{3}, \quad \frac{\Delta\mathcal{N}_n^{\pi^-}}{\mathcal{N}_n^{\pi^-}} = \frac{2}{3}. \quad (9b)$$

Finally, for ratios of neutron to proton cross sections with either π^+ or π^- we have:

$$\frac{\mathcal{N}_n^{\pi^+}}{\mathcal{N}_p^{\pi^+}} = \frac{\mathcal{N}_p^{\pi^-}}{\mathcal{N}_n^{\pi^-}} = \frac{1}{2}, \quad (10a)$$

$$\frac{\mathcal{N}_n^{\pi^-}}{\mathcal{N}_p^{\pi^-}} = \frac{\mathcal{N}_p^{\pi^+}}{\mathcal{N}_n^{\pi^+}} = 4. \quad (10b)$$

This is consistent with the parton model results for ratios of parton distributions satisfying SU(6) symmetry [3,6], $d/u = 1/2$, $\Delta u/u = 2/3$, $\Delta d/d = -1/3$, $\Delta d/\Delta u = -1/4$, confirming the validity of duality for the case $\bar{D} = 0$, as in Eq.(2).

Furthermore, the inclusive results of Ref. [3] can be recovered by summing over the π^+ and π^- channels. In this case one finds the familiar results

$$\frac{\mathcal{N}_n^{\pi^+ + \pi^-}}{\mathcal{N}_p^{\pi^+ + \pi^-}} = \frac{F_1^n}{F_1^p} = \frac{2}{3}, \quad (11a)$$

$$\frac{\Delta\mathcal{N}_p^{\pi^+ + \pi^-}}{\mathcal{N}_p^{\pi^+ + \pi^-}} = \frac{g_1^p}{F_1^p} = \frac{5}{9}, \quad (11b)$$

$$\frac{\Delta\mathcal{N}_n^{\pi^+ + \pi^-}}{\mathcal{N}_n^{\pi^+ + \pi^-}} = \frac{g_1^n}{F_1^n} = 0, \quad (11c)$$

again consistent with the parton-level expectations.

B. Spin-1/2 dominance

Although the SU(6) symmetric results may be expected to be approximately valid for structure functions at $x \sim 1/3$, at larger x values strong deviations from SU(6) symmetry are observed. These can be correlated with SU(6)-breaking effects in the transition form factors, as well as in hadron masses. It is well known that spin-dependent forces between quarks, such as from one gluon exchange [16], introduce a mass difference between the nucleon and Δ . The same mechanism also leads to an anomalous suppression of the $N \rightarrow \Delta$ transition form factor relative to the nucleon elastic at high Q^2 [17,18].

If the characteristic Q^2 suppression of the Δ excitation is related with the spin dependence, then it may be a feature of all $S = 3/2$ states, namely the [**410, 56⁺**] and [**48, 70⁻**]. In fact, in the approximation of magnetic coupling dominance, which is more accurate with increasing Q^2 , only $S = 3/2$

configurations allow nonzero $\sigma_{3/2}$ cross sections. Suppression of these then automatically gives unity for the polarized to unpolarized ratios,

$$\frac{\Delta \mathcal{N}_N^\pi}{\mathcal{N}_N^\pi} = 1. \quad (12)$$

For the unpolarized ratios, including only the ${}^2\mathbf{8}$ and ${}^2\mathbf{10}$ contributions, the π^- to π^+ ratios for the proton and neutron become:

$$\frac{\mathcal{N}_p^{\pi^-}}{\mathcal{N}_p^{\pi^+}} = \frac{1}{56}, \quad \frac{\mathcal{N}_n^{\pi^-}}{\mathcal{N}_n^{\pi^+}} = \frac{7}{2}. \quad (13)$$

At the parton level, these results imply the ratio $\Delta q/q = 1$ for $q = u$ and d and a flavor-dependent ratio of down to up quark distributions $d/u = 1/14$. This is consistent with the findings of the inclusive duality study in Ref. [6], confirming the duality between the parton- and hadron-level descriptions of the semi-inclusive scattering process also.

C. Scalar diquark dominance

If the mass difference between the nucleon and Δ is attributed to spin-dependent forces, the energy associated with the symmetric part of the nucleon wave function will be larger than that of the antisymmetric component. At the quark level, this pattern of suppression can be realized with a spin-dependent hyperfine interaction between quarks, $\vec{S}_i \cdot \vec{S}_j$, which modifies the spin-0 and spin-1 components of the nucleon wave function. Physically this correlates with a ‘‘diquark’’ in a $q(qq)$ representation of the nucleon having a larger mass (energy) when the spin of the qq pair is 1. A suppression of the symmetric configuration at large x will then give rise to a softening of the d quark distribution relative to the u and leads to the proton and neutron polarization asymmetries becoming unity as $x \rightarrow 1$ [13,17].

In terms of the SU(6) representations, the ${}^2\mathbf{10}$ and ${}^4\mathbf{8}$ multiplets are in the ${}^{\mathbf{70}^-}$ and the ${}^{\mathbf{410}}$ unambiguously in the ${}^{\mathbf{56}^+}$ representation. However, the spin-1/2 ${}^2\mathbf{8}$ can occur in both the ${}^{\mathbf{56}^+}$ and ${}^{\mathbf{70}^-}$ representations and can be written in terms of symmetric ψ_λ and antisymmetric ψ_ρ components, where $\psi = \varphi \otimes \chi$ is a product of the flavor (φ) and spin (χ) wave functions and λ and ρ denote the symmetric and antisymmetric combinations, respectively [19]. In the SU(6) limit one has an equal admixture of both ρ - and λ -type contributions, whereas in the present scenario only the ρ components in the ${}^{\mathbf{56}^+}$ and ${}^{\mathbf{70}^-}$ multiplets plays a role. In particular, because transitions to the (symmetric) spin-3/2 states (${}^{\mathbf{48}}$, ${}^{\mathbf{410}}$, and ${}^{\mathbf{210}}$) can proceed only through the symmetric λ component of the ground-state wave function, the ρ components will excite only the nucleon to ${}^2\mathbf{8}$ states. If the λ wave function is suppressed, only transitions to ${}^2\mathbf{8}$ states will be allowed.

To effect this scenario, the simplest strategy is to sum coherently the ${}^2\mathbf{8}$ amplitudes in the intermediate N_1^* states and in the final N_2^* states in Tables III and V, before squaring the result to get the cross section. Doing so one finds that π^- production from the proton and π^+ production from the neutron are both suppressed:

$$\frac{\mathcal{N}_p^{\pi^-}}{\mathcal{N}_p^{\pi^+}} = 0, \quad \frac{\mathcal{N}_n^{\pi^+}}{\mathcal{N}_n^{\pi^-}} = 0, \quad (14)$$

with the ratio of the unsuppressed yields being:

$$\frac{\mathcal{N}_n^{\pi^-}}{\mathcal{N}_p^{\pi^+}} = \frac{1}{4}. \quad (15)$$

These results are consistent with parton model results in which $d/u \rightarrow 0$ as $x \rightarrow 1$. Finally, because the ${}^2\mathbf{8}$ amplitudes have no helicity-3/2 components, the spin-dependent semi-inclusive cross sections will be identical to the spin-averaged ones, with all polarization asymmetries unity, again as in the parton-level model.

D. Helicity-1/2 dominance

The central tenet of quark-hadron duality is the nontrivial relationship between the behavior of structure functions at large x and that of transition form factors at high Q^2 . At high Q^2 perturbative QCD arguments suggest that the interaction of the photon should be predominantly with quarks having the same helicity as the nucleon [20,21]. Because the scattering of a photon from a massless quark conserves helicity, the helicity-3/2 amplitude $A_{3/2}$ would be expected to be suppressed relative to the $A_{1/2}$ [19].

In Ref. [6] duality was demonstrated to exist between parton distributions at large x and resonance transitions classified according to quark *helicity* rather than spin. Here we examine whether this duality extends also to the semi-inclusive case with helicity-1/2 dominance. Table II lists the relative weights of the $\gamma N \rightarrow N_1^* \rightarrow \pi N_2^*$ transitions (scaled by a factor $9^2 = 81$), summed over intermediate states N_1^* , in this scenario. The results are obtained by suppressing all helicity-3/2 amplitudes $A_{3/2}$ in Tables III–VII for both the N_1^* and N_2^* states. The results for the spin-averaged and spin-dependent transitions are therefore identical.

The ratios of π^- to π^+ cross sections for proton and neutron targets in this scenario are given by:

$$\frac{\mathcal{N}_p^{\pi^-}}{\mathcal{N}_p^{\pi^+}} = \frac{1}{20}, \quad \frac{\mathcal{N}_n^{\pi^-}}{\mathcal{N}_n^{\pi^+}} = \frac{5}{4}. \quad (16)$$

Furthermore, the neutron-to-proton ratios for π^\pm production are given by:

$$\frac{\mathcal{N}_n^{\pi^+}}{\mathcal{N}_p^{\pi^+}} = \frac{\mathcal{N}_p^{\pi^-}}{\mathcal{N}_n^{\pi^-}} = \frac{1}{5}, \quad (17)$$

TABLE II. Relative strengths of the $\gamma N \rightarrow N_1^* \rightarrow \pi N_2^*$ transitions for the F_1 or g_1 structure function in the helicity-1/2 dominance model, after summing over all intermediate states N_1^* .

	N_2^*					Sum
	${}^2\mathbf{8}, \mathbf{56}^+$	${}^{\mathbf{410}}, \mathbf{56}^+$	${}^2\mathbf{8}, \mathbf{70}^-$	${}^{\mathbf{48}}, \mathbf{70}^-$	${}^{\mathbf{210}}, \mathbf{70}^-$	
$\gamma p \rightarrow \pi^+ N_2^*$	100	8	64	4	4	180
$\gamma p \rightarrow \pi^- N_2^*$	0	6	0	0	3	9
$\gamma n \rightarrow \pi^+ N_2^*$	0	24	0	0	12	36
$\gamma n \rightarrow \pi^- N_2^*$	25	2	16	1	1	45

and for consistency one can also verify that

$$\frac{\mathcal{N}_n^{\pi^+}}{\mathcal{N}_p^{\pi^+}} = \frac{\mathcal{N}_n^{\pi^-}}{\mathcal{N}_p^{\pi^-}} = 4. \quad (18)$$

These results are consistent with the parton model predictions for helicity-1/2 dominance [20], which yield $d/u = 1/5$.

Suppression of the helicity-3/2 contributions means that the spin-dependent semi-inclusive cross sections are identical to the spin-averaged,

$$\frac{\Delta \mathcal{N}_N^\pi}{\mathcal{N}_N^\pi} = 1. \quad (19)$$

This again is consistent with the parton model calculations that predict that $\Delta q/q = 1$ for all quark flavors q [20].

IV. COMPARISON WITH DATA

Recently the onset of duality in pion electroproduction was studied in scattering from proton and deuteron targets [7], with the missing mass M_2^* of the residual system spanning the resonance region. Ratios of π^+ to π^- cross sections were found to exhibit features reminiscent of parton-level factorization of the hard scattering and subsequent fragmentation processes, even at relatively low energies. In addition, the ratio of unfavored to favored fragmentation functions was found to closely resemble that observed at much higher energies from earlier experiments by HERMES [9] and EMC [10].

As noted in Ref. [7], some of the qualitative features of the data could be understood in the simple quark model discussed in Ref. [3] (and in Sec. III above). In particular, for a deuteron target the resonance contributions to the π^+/π^- ratio appear in a universal 4:1 ratio when summed over the 56^+ and 70^- multiplets and cancel in the ratio of unfavored to favored fragmentation functions $R \equiv \overline{D}/D$, leaving only a smooth background as expected at higher energies. The absence of strong resonant enhancement on top of the smooth background is indeed one of the notable features of the data [7].

Although the lack of prominent N^* structure in the semi-inclusive spectrum is in accord with duality, a quantitative comparison goes beyond the simple model discussed thus far. In our model an operator equivalent to $u \rightarrow \pi^+ d$ is sandwiched between SU(6) states for N_1^* and N_2^* , after which the initial and final states are summed over (see Appendix B). This mechanism allows only for leading fragmentation to take place, whereas the data [7] clearly show that for $z < 1$ the ratio $R \neq 0$. The model can therefore only be applied to the resonance part of the semi-inclusive cross section and is not applicable to the nonresonant background, which makes up a sizable fraction of the data at $z \ll 1$.

The simplest generalization of this formalism to the case of $R \neq 0$ is to retain the assumption that the pion production operator factors from the initial and final N^* but allow the possibility that the u quark, for instance, can fragment to a π^- . An example of such a mechanism would be $u \rightarrow M^+ X$, where M^+ is some heavy resonance, followed by the decay $M^+ \rightarrow \pi^+ \pi^+ \pi^-$, leaving the baryonic state X unaltered. This can be accommodated phenomenologically by assuming, as in Ref. [3], that the ratio R is independent of N^* . The

relative contributions from the various N_2^* states to the semi-inclusive cross section for the \overline{D} contribution then follow immediately by interchanging $\pi^+ \longleftrightarrow \pi^-$ in each column of Tables III–VII.

In the particular case of a deuteron target the ratio of π^+ to π^- cross sections generalizes to

$$\frac{\mathcal{N}_d^{\pi^+}}{\mathcal{N}_d^{\pi^-}} = \frac{4 + R}{4R + 1}, \quad (20)$$

and is in fact the same for each multiplet $N_2^* = [28, 56^+]$, $[410, 56^+]$, $[28, 70^-]$, $[48, 70^-]$, or $[210, 70^-]$, as well as of course for the sum. Inverting Eq. (20), we find the ratio

$$R = \frac{4 - \mathcal{N}_d^{\pi^+}/\mathcal{N}_d^{\pi^-}}{4\mathcal{N}_d^{\pi^+}/\mathcal{N}_d^{\pi^-} - 1}, \quad (21)$$

which clearly vanishes in the limit when $\mathcal{N}_d^{\pi^+} = 4\mathcal{N}_d^{\pi^-}$. Interestingly, the 4:1 ratio is realized not only for the SU(6) symmetric model but also for the various SU(6)-breaking scenarios discussed in Sec. III. To discriminate between the different symmetry-breaking mechanisms, it is therefore not sufficient to simply extend the kinematics to the large- x region with a deuteron target; one must consider explicitly proton (or neutron) targets, where the different symmetry-breaking models yield very different π^+/π^- predictions—see Eqs. (7), (13), (14), and (16).

Experimentally, the presence of secondary, or unfavored, fragmentation gives a sizable contribution to the semi-inclusive cross section and dilutes the simple predictions for the π^+ -to- π^- ratios derived in Sec. III. However, even though a quantitative comparison of the ratios may at present be beyond reach, some general features of the data can nevertheless be understood within the favored fragmentation scenario.

For a proton target, the empirical ratio $\mathcal{N}_p^{\pi^+}/\mathcal{N}_p^{\pi^-}$ is found to be ≈ 2 for $0.3 \lesssim z \lesssim 0.7$, as seen in Fig. 1 for fixed $x = 0.32$ and $Q^2 \approx 2.5 \text{ GeV}^2$ [2,22]. This is to be compared with a π^+/π^- ratio of eight predicted in the SU(6) model when $z \rightarrow 1$, Eq. (7). A careful examination of the data [22] at larger x further reveals a clear trend in which the π^+/π^- ratio increases with increasing x , consistent with the expectations of the symmetry-breaking scenarios. For example, the helicity 1/2 dominance model predicts a π^+/π^- ratio of 20 [Eq. (16)], the spin 1/2 dominance model gives 56 [Eq. (13)], while the scalar diquark model yields a divergent ratio [Eq. (14)]. Of course to discriminate among these predictions requires data at larger x ($x \sim 1$) than is currently available, which will be an important challenge for future experiments.

For deuterium targets, the empirical $\mathcal{N}_d^{\pi^+}/\mathcal{N}_d^{\pi^-}$ ratio is found to be around 1.5 [7], compared with the model prediction of 4, in both the SU(6) symmetric model and in the various symmetry-breaking extensions. As for the proton, the trend of the deuteron data is an increase of this ratio with increasing x .

Because nuclear effects in the deuteron at $x \sim 0.3$ are small [23], the π^+/π^- ratios for a neutron target can be extracted from the difference of the deuteron and proton data, as shown in Fig. 1. Here the $\mathcal{N}_n^{\pi^+}/\mathcal{N}_n^{\pi^-}$ ratio is close to unity and considerably smaller than the proton ratio. In the SU(6)

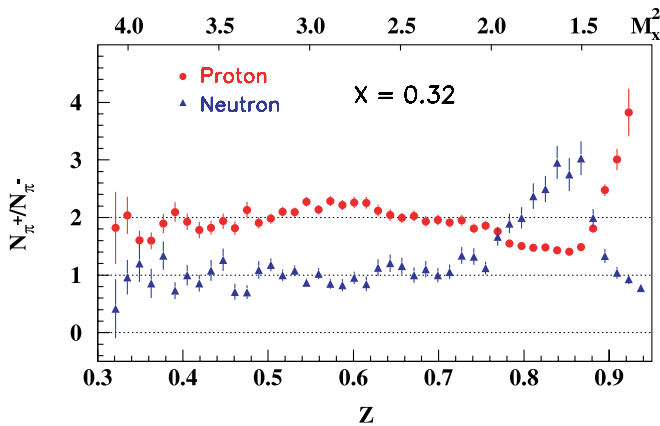


FIG. 1. (Color online) Ratio N^{π^+}/N^{π^-} for proton (circles) and “neutron” (triangles) targets from Jefferson Lab Hall C [7,22], as a function of z (and $M_x^2 \equiv M_2^*$, in units of GeV^2 , upper scale), at fixed $x = 0.32$ and $Q^2 \approx 2.5 \text{ GeV}^2$.

quark model the expectation for the ratio is 2, Eq. (7), so that again the data suggest a dilution of the primary fragmentation mechanism of π^\pm production.

At larger z (or smaller M_2^*), the nucleon resonance structures become more apparent in both the proton and neutron data. Because secondary fragmentation is suppressed as $z \rightarrow 1$, we may expect the nonresonant background to play a lesser role here and the predictions of the resonance model of Sec. III to be more quantitative. In the Δ resonance region, for example, at $0.8 \lesssim z \lesssim 0.85$ ($M_2^* \approx 1.2 - 1.3 \text{ GeV}$), the proton ratio dips to about 1.5, while the neutron ratio increases severalfold and becomes larger than the proton. This behavior is expected from the relative strengths of the transitions for the $[410, 56^+]$ multiplet in Tables I and II, in which the neutron $\rightarrow \Delta^0$ transitions are predicted to be an order of magnitude larger than for the proton $\rightarrow \Delta^+$.

For even larger z the proton and neutron ratios are inverted again and display rather different behaviors in the limit $z \rightarrow 1$, which corresponds to a nucleon elastic final state, $N_2^* = N$. Because only π^+ production is possible from the proton, and π^- from the neutron, the ratio of π^+ to π^- rises steeply for the proton but drops rapidly to zero for the neutron [2]. Again this trend is consistent with the quark model expectations from Sec. III, whose predictions should be more robust in this region.

V. CONCLUSION

In this study we have shown how the quark-hadron duality that was successfully demonstrated for inclusive structure functions in the quark model [3] can be extended to semi-inclusive pion electroproduction, with corresponding patterns of resonances that are dual to the parton model results. Having derived the full set of matrix elements for $\gamma N \rightarrow N_1^* \rightarrow \pi N_2^*$, where both N_1^* and N_2^* belong to the 56^+ and 70^- multiplets of SU(6), we demonstrated duality by comparing the hadronic-level results, summed over the $N_{1,2}^*$, with those of the parton model. In the case of spin-flavor symmetry, these are most immediately applicable when $x \sim 1/3$ and in

the leading fragmentation approximation, which is valid at large z , where secondary fragmentation is suppressed.

We find that duality is indeed realized even in the broken SU(6) case, in the sense that sums over resonances are able to reproduce parton model semi-inclusive cross-section ratios. In Ref. [6] it was shown how duality for inclusive structure functions could be realized in various SU(6)-breaking scenarios; here we have shown how duality is realized in these scenarios for semi-inclusive pion electroproduction as $x \rightarrow 1$. The different patterns of resonances N_2^* and ratios of π^+/π^- may be used to isolate the dynamics of symmetry breaking in the $x \rightarrow 1$ regime.

Comparisons with data show that this analysis gives a qualitative description of the features and general trends of the data, especially at large z . Although the results of Ref. [3] were obtained in the leading fragmentation approximation, which is valid at large z , quantitative comparison with data at intermediate z values requires including subleading fragmentation, characterized by nonzero values of the fragmentation function ratio \bar{D}/D . We have shown how to incorporate the effects of $\bar{D}/D \neq 0$ phenomenologically in a way consistent with duality, although the z dependence is a model-dependent effect that goes beyond the present work and does not follow from duality alone.

Although future precision semi-inclusive studies at large x will be challenging experimentally, they will be vital in providing constraints on the flavor and spin dependence of quark interactions in the nucleon, complementary to those from inclusive measurements. In this regard a program of polarized semi-inclusive deep-inelastic scattering to measure spin-dependent cross section ratios would also be extremely valuable, allowing direct tests of the predictions presented in this work.

On the theoretical front, quantitative comparison with data at low Q^2 and large x and z will require implementation of semi-inclusive target mass corrections [24], as well as nuclear effects when considering nuclear data at large x [23]. For a systematic analysis of the full z dependence of semi-inclusive cross sections, the present model needs to be extended to include a microscopic, quark-level description of unfavored fragmentation, $\bar{D}/D \neq 0$. This would then enable predictions to be made for the angular or p_T dependence of semi-inclusive pion production [8], which may reveal further insights into the hadronization process.

ACKNOWLEDGMENTS

We are indebted to R. Ent and H. Mkrtychyan for helpful communications about the semi-inclusive data from Hall C at Jefferson Lab [7]. W.M. is supported by the DOE Contract No. DE-AC05-06OR23177, under which Jefferson Science Associates, LLC operates Jefferson Lab. F.E.C. is supported in part by grants from the Science & Technology Facilities Council (UK).

APPENDIX A: $\gamma N \rightarrow \pi N_2^*$ AMPLITUDES

In this Appendix we present for completeness the full set of amplitudes for the transitions $\gamma N \rightarrow N_1^* \rightarrow \pi N_2^*$, for $N = p$ and n targets. In Tables III–VII we give the relative weights

TABLE III. Relative strengths of the helicity 1/2 and 3/2 transition amplitudes for $\gamma N \rightarrow N_1^* \rightarrow \pi N_2^*$ for the $N_2^* = [{}^2\mathbf{8}, \mathbf{56}^+]$ multiplet.

N_1^*	$\gamma p \rightarrow \pi^+ N_2^*$		$\gamma p \rightarrow \pi^- N_2^*$		$\gamma n \rightarrow \pi^+ N_2^*$		$\gamma n \rightarrow \pi^- N_2^*$	
	$A_{1/2}$	$A_{3/2}$	$A_{1/2}$	$A_{3/2}$	$A_{1/2}$	$A_{3/2}$	$A_{1/2}$	$A_{3/2}$
${}^2\mathbf{8}, \mathbf{56}^+$	$\frac{5}{9}$	0	0	0	0	0	$-\frac{10}{27}$	0
${}^4\mathbf{10}, \mathbf{56}^+$	$\frac{4}{27}$	0	0	0	0	0	$-\frac{4}{27}$	0
${}^2\mathbf{8}, \mathbf{70}^-$	$\frac{4}{9}$	0	0	0	0	0	$-\frac{4}{27}$	0
${}^4\mathbf{8}, \mathbf{70}^-$	0	0	0	0	0	0	$\frac{2}{27}$	0
${}^2\mathbf{10}, \mathbf{70}^-$	$-\frac{1}{27}$	0	0	0	0	0	$\frac{1}{27}$	0

TABLE IV. Relative strengths of the helicity 1/2 and 3/2 transition amplitudes for $\gamma N \rightarrow N_1^* \rightarrow \pi N_2^*$ for the $N_2^* = [{}^4\mathbf{10}, \mathbf{56}^+]$ multiplet.

N_1^*	$\gamma p \rightarrow \pi^+ N_2^*$		$\gamma p \rightarrow \pi^- N_2^*$		$\gamma n \rightarrow \pi^+ N_2^*$		$\gamma n \rightarrow \pi^- N_2^*$	
	$A_{1/2}$	$A_{3/2}$	$A_{1/2}$	$A_{3/2}$	$A_{1/2}$	$A_{3/2}$	$A_{1/2}$	$A_{3/2}$
${}^2\mathbf{8}, \mathbf{56}^+$	$\frac{2\sqrt{2}}{9}$	0	$-\frac{2}{3}\sqrt{\frac{2}{3}}$	0	$-\frac{4}{9}\sqrt{\frac{2}{3}}$	0	$\frac{4\sqrt{2}}{27}$	0
${}^4\mathbf{10}, \mathbf{56}^+$	$-\frac{2\sqrt{2}}{27}$	$-\frac{2}{3}\sqrt{\frac{2}{3}}$	$-\frac{1}{9}\sqrt{\frac{2}{3}}$	$-\frac{\sqrt{2}}{3}$	$-\frac{1}{9}\sqrt{\frac{2}{3}}$	$-\frac{\sqrt{2}}{3}$	$-\frac{2\sqrt{2}}{27}$	$-\frac{2}{3}\sqrt{\frac{2}{3}}$
${}^2\mathbf{8}, \mathbf{70}^-$	$-\frac{2\sqrt{2}}{9}$	0	$\frac{2}{3}\sqrt{\frac{2}{3}}$	0	$\frac{2}{9}\sqrt{\frac{2}{3}}$	0	$-\frac{2\sqrt{2}}{27}$	0
${}^4\mathbf{8}, \mathbf{70}^-$	0	0	0	0	$-\frac{1}{9}\sqrt{\frac{2}{3}}$	$-\frac{\sqrt{2}}{3}$	$\frac{\sqrt{2}}{27}$	$\frac{1}{3}\sqrt{\frac{2}{3}}$
${}^2\mathbf{10}, \mathbf{70}^-$	$-\frac{4\sqrt{2}}{27}$	0	$-\frac{2}{9}\sqrt{\frac{2}{3}}$	0	$-\frac{2}{9}\sqrt{\frac{2}{3}}$	0	$-\frac{4\sqrt{2}}{27}$	0

TABLE V. Relative strengths of the helicity 1/2 and 3/2 transition amplitudes for $\gamma N \rightarrow N_1^* \rightarrow \pi N_2^*$ for the $N_2^* = [{}^2\mathbf{8}, \mathbf{70}^-]$ multiplet.

N_1^*	$\gamma p \rightarrow \pi^+ N_2^*$		$\gamma p \rightarrow \pi^- N_2^*$		$\gamma n \rightarrow \pi^+ N_2^*$		$\gamma n \rightarrow \pi^- N_2^*$	
	$A_{1/2}$	$A_{3/2}$	$A_{1/2}$	$A_{3/2}$	$A_{1/2}$	$A_{3/2}$	$A_{1/2}$	$A_{3/2}$
${}^2\mathbf{8}, \mathbf{56}^+$	$\frac{4}{9}$	0	0	0	0	0	$-\frac{8}{27}$	0
${}^4\mathbf{10}, \mathbf{56}^+$	$-\frac{4}{27}$	0	0	0	0	0	$\frac{4}{27}$	0
${}^2\mathbf{8}, \mathbf{70}^-$	$\frac{5}{9}$	0	0	0	0	0	$-\frac{5}{27}$	0
${}^4\mathbf{8}, \mathbf{70}^-$	0	0	0	0	0	0	$-\frac{2}{27}$	0
${}^2\mathbf{10}, \mathbf{70}^-$	$\frac{1}{27}$	0	0	0	0	0	$-\frac{1}{27}$	0

TABLE VI. Relative strengths of the helicity 1/2 and 3/2 transition amplitudes for $\gamma N \rightarrow N_1^* \rightarrow \pi N_2^*$ for the $N_2^* = [{}^4\mathbf{8}, \mathbf{70}^-]$ multiplet.

N_1^*	$\gamma p \rightarrow \pi^+ N_2^*$		$\gamma p \rightarrow \pi^- N_2^*$		$\gamma n \rightarrow \pi^+ N_2^*$		$\gamma n \rightarrow \pi^- N_2^*$	
	$A_{1/2}$	$A_{3/2}$	$A_{1/2}$	$A_{3/2}$	$A_{1/2}$	$A_{3/2}$	$A_{1/2}$	$A_{3/2}$
${}^2\mathbf{8}, \mathbf{56}^+$	$\frac{2}{9}$	0	0	0	0	0	$\frac{4}{27}$	0
${}^4\mathbf{10}, \mathbf{56}^+$	$\frac{2}{27}$	$\frac{2}{3\sqrt{3}}$	0	0	0	0	$-\frac{2}{27}$	$-\frac{2}{3\sqrt{3}}$
${}^2\mathbf{8}, \mathbf{70}^-$	$-\frac{2}{9}$	0	0	0	0	0	$-\frac{2}{27}$	0
${}^4\mathbf{8}, \mathbf{70}^-$	0	0	0	0	0	0	$\frac{1}{27}$	$\frac{1}{3\sqrt{3}}$
${}^2\mathbf{10}, \mathbf{70}^-$	$\frac{4}{27}$	0	0	0	0	0	$-\frac{4}{27}$	0

TABLE VII. Relative strengths of the helicity 1/2 and 3/2 transition amplitudes for $\gamma N \rightarrow N_1^* \rightarrow \pi N_2^*$ for the $N_2^* = [{}^2\mathbf{10}, \mathbf{70}^-]$ multiplet.

N_1^*	$\gamma p \rightarrow \pi^+ N_2^*$		$\gamma p \rightarrow \pi^- N_2^*$		$\gamma n \rightarrow \pi^+ N_2^*$		$\gamma n \rightarrow \pi^- N_2^*$	
	$A_{1/2}$	$A_{3/2}$	$A_{1/2}$	$A_{3/2}$	$A_{1/2}$	$A_{3/2}$	$A_{1/2}$	$A_{3/2}$
${}^2\mathbf{8}, \mathbf{56}^+$	$-\frac{1}{9}$	0	$-\frac{1}{3\sqrt{3}}$	0	$\frac{2}{9\sqrt{3}}$	0	$-\frac{2}{27}$	0
${}^4\mathbf{10}, \mathbf{56}^+$	$-\frac{8}{27}$	0	$-\frac{4}{9\sqrt{3}}$	0	$-\frac{4}{9\sqrt{3}}$	0	$-\frac{8}{27}$	0
${}^2\mathbf{8}, \mathbf{70}^-$	$\frac{1}{9}$	0	$\frac{1}{3\sqrt{3}}$	0	$-\frac{1}{9\sqrt{3}}$	0	$\frac{1}{27}$	0
${}^4\mathbf{8}, \mathbf{70}^-$	0	0	0	0	$-\frac{4}{9\sqrt{3}}$	0	$\frac{4}{27}$	0
${}^2\mathbf{10}, \mathbf{70}^-$	$\frac{2}{27}$	0	$\frac{1}{9\sqrt{3}}$	0	$\frac{1}{9\sqrt{3}}$	0	$\frac{2}{27}$	0

for the helicity amplitudes $A_{1/2}$ and $A_{3/2}$ for individual N_1^* intermediate states and N_2^* final states spanning the $\mathbf{56}^+$ and $\mathbf{70}^-$ multiplets. We follow the notations of Refs. [11,19,25], but with a different sign convention for the Clebsch-Gordan coefficients to that of the Particle Data Group [26] (the results for the cross sections do not depend on the convention however).

APPENDIX B: SAMPLE MATRIX ELEMENT COMPUTATION

We provide here an example of a calculation of a typical matrix element in Tables III–VII in the SU(6) quark model. To be specific we consider the octet states symmetric and antisymmetric parts are labeled λ and ρ . The spin-1/2 octets in the $\mathbf{56}^+$ and $\mathbf{70}^-$ multiplets are written

$$[{}^2\mathbf{8}, \mathbf{56}^+] = \frac{1}{\sqrt{2}}(\phi_\rho \chi_\rho + \phi_\lambda \chi_\lambda), \quad (\text{B1})$$

$$[{}^2\mathbf{8}, \mathbf{70}^-] = \frac{1}{\sqrt{2}}(\phi_\rho \chi_\rho - \phi_\lambda \chi_\lambda), \quad (\text{B2})$$

where ϕ and χ denote the flavor and spin wave functions, respectively, explicit forms for which can be found in Refs. [19, 25]. Note that in this convention the state with a scalar diquark can be written as $|\phi_\rho \chi_\rho\rangle = \{|{}^2\mathbf{8}, \mathbf{56}^+\rangle + |{}^2\mathbf{8}, \mathbf{70}^-\rangle\}/\sqrt{2}$.

Consider the process $\gamma N \rightarrow N_1^*$, with the nucleon at rest and the photon along the \hat{z} axis with $J_z = +1$. The helicity amplitude $A_{1/2}$ then corresponds to a nucleon having $J_z = -1/2$, leaving the N_1^* with $J_z = +1/2$. In the limit of magnetic coupling (corresponding to spin-flip), the electromagnetic current J^{em} transforms as $\sum_i e_i \sigma_i^+$, summed over the three

valence quarks. For a proton target, because the matrix elements of this operator are unity for the $\phi_\rho \chi_\rho$ component and zero for the $\phi_\lambda \chi_\lambda$ components, one has

$$\langle {}^2\mathbf{8}, \mathbf{56}^+ | J^{\text{em}} | {}^2\mathbf{8}, \mathbf{56}^+ \rangle = \langle {}^2\mathbf{8}, \mathbf{70}^- | J^{\text{em}} | {}^2\mathbf{8}, \mathbf{56}^+ \rangle = 1. \quad (\text{B3})$$

Now consider the decay of a positively charged state N_1^* to a π^+ and a neutral baryon N_2^* , with both the N_1^* and N_2^* states in either the $[{}^2\mathbf{8}, \mathbf{56}^+]$ or $[{}^2\mathbf{8}, \mathbf{70}^-]$ multiplets. Assuming that the π^+ is emitted collinearly along the γN axis, which is valid in the $z \rightarrow 1$ limit, the π^+ emission operator transforms as $J^\pi = \tau^- \sigma_z$. After summing over the three valence quarks, one has the matrix elements

$$\langle \phi_\lambda \chi_\lambda | \tau^- \sigma_z | \phi_\lambda \chi_\lambda \rangle = \frac{1}{9}, \quad (\text{B4a})$$

$$\langle \phi_\rho \chi_\rho | \tau^- \sigma_z | \phi_\rho \chi_\rho \rangle = \frac{1}{9}, \quad (\text{B4b})$$

from which one derives the transition matrix elements

$$\langle {}^2\mathbf{8}, \mathbf{56}^+ | J^\pi | {}^2\mathbf{8}, \mathbf{56}^+ \rangle = \langle {}^2\mathbf{8}, \mathbf{70}^- | J^\pi | {}^2\mathbf{8}, \mathbf{70}^- \rangle = \frac{5}{9}, \quad (\text{B5a})$$

$$\langle {}^2\mathbf{8}, \mathbf{56}^+ | J^\pi | {}^2\mathbf{8}, \mathbf{70}^- \rangle = \langle {}^2\mathbf{8}, \mathbf{70}^- | J^\pi | {}^2\mathbf{8}, \mathbf{56}^+ \rangle = \frac{4}{9}. \quad (\text{B5b})$$

The product of the matrix elements of J^{em} and J^π then give the entries in Tables III and V. For example, for the transition $\gamma N \rightarrow N_1^* [{}^2\mathbf{8}, \mathbf{70}^-] \rightarrow \pi N_2^* [{}^2\mathbf{8}, \mathbf{56}^+]$ one has

$$\langle {}^2\mathbf{8}, \mathbf{56}^+ | J^\pi | {}^2\mathbf{8}, \mathbf{70}^- \rangle \cdot \langle {}^2\mathbf{8}, \mathbf{70}^- | J^{\text{em}} | {}^2\mathbf{8}, \mathbf{56}^+ \rangle = \frac{4}{9}, \quad (\text{B6})$$

as given in Table III.

- [1] E. D. Bloom and F. J. Gilman, Phys. Rev. Lett. **25**, 1140 (1970).
- [2] W. Melnitchouk, R. Ent, and C. Keppel, Phys. Rep. **406**, 127 (2005).
- [3] F. E. Close and N. Isgur, Phys. Lett. **B509**, 81 (2001).
- [4] N. Isgur, S. Jeschonnek, W. Melnitchouk, and J. W. Van Orden, Phys. Rev. D **64**, 054005 (2001).
- [5] M. W. Paris and V. R. Pandharipande, Phys. Lett. **B514**, 361 (2001); Phys. Rev. C **65**, 035203 (2002); S. Jeschonnek and J. W. Van Orden, Phys. Rev. D **65**, 094038 (2002); F. E. Close and Q. Zhao, *ibid.* **66**, 054001 (2002).

- [6] F. E. Close and W. Melnitchouk, Phys. Rev. C **68**, 035210 (2003).
- [7] T. Navasardyan *et al.*, Phys. Rev. Lett. **98**, 022001 (2007).
- [8] H. Mkrtchyan *et al.*, Phys. Lett. **B665**, 20 (2008).
- [9] P. Geiger, Ph.D. thesis, Heidelberg University, 1998; B. Hommez, Ph.D. thesis, Gent University, 2003.
- [10] M. Arneodo *et al.*, Nucl. Phys. **B321**, 541 (1989).
- [11] A. Afanasev, C. E. Carlson, and C. Wahlquist, Phys. Rev. D **62**, 074011 (2000).
- [12] P. Hoyer, in *Exclusive Processes at High Momentum Transfer* (Newport News, Virginia, 2002), arXiv:hep-ph/0208190.

- [13] F. E. Close, Nucl. Phys. **B80**, 269 (1974).
- [14] F. E. Close and F. J. Gilman, Phys. Lett. **B38**, 541 (1972).
- [15] F. E. Close, H. Osborn, and A. M. Thomson, Nucl. Phys. **B77**, 281 (1974).
- [16] A. De Rújula, H. Georgi, and S. L. Glashow, Phys. Rev. D **12**, 147 (1975).
- [17] F. E. Close, Phys. Lett. **B43**, 422 (1973).
- [18] P. Stoler, Phys. Rev. D **44**, 73 (1991).
- [19] F. E. Close, *Introduction to Quarks and Partons* (Academic Press, London, 1979).
- [20] G. R. Farrar and D. R. Jackson, Phys. Rev. Lett. **35**, 1416 (1975).
- [21] J. F. Gunion, P. Nason, and R. Blankenbecler, Phys. Rev. D **29**, 2491 (1984).
- [22] H. Mkrtchyan (private communication).
- [23] W. Melnitchouk, J. Speth, and A. W. Thomas, Phys. Lett. **B435**, 420 (1998).
- [24] A. Accardi, T. Hobbs, and W. Melnitchouk (in preparation).
- [25] N. Isgur and G. Karl, Phys. Rev. D **18**, 4187 (1978).
- [26] C. Amsler *et al.*, Phys. Lett. **B667**, 1 (2008).